Ore Geology Reviews 120 (2020) 103397

Contents lists available at ScienceDirect

Ore Geology Reviews

journal homepage: www.elsevier.com/locate/oregeorev

Geostatistics in the presence of geological boundaries: Exploratory tools for contact analysis

Mohammad Maleki[a,*], Xavier Emery[b,c]

[a] Department of Metallurgical and Mining Engineering, Universidad Católica del Norte, Antofagasta, Chile
[b] Department of Mining Engineering, University of Chile, Santiago, Chile
[c] Advanced Mining Technology Center, University of Chile, Santiago, Chile

ARTICLE INFO

Keywords:
Cross-to-direct variogram ratios
Cross-correlograms
Pseudo cross-variograms
Lagged scatter plots
Partial grades
Hard and soft boundaries

ABSTRACT

Identification and categorization of geological, geotechnical, or geometallurgical domains is a common practice in the modeling of mineral deposits, in order to account for the controls exerted by categorical variables (ore type, rock type or facies) on the quantitative variables of interest. The definition of a suitable geostatistical model for spatial prediction or simulation is commonly based on a contact analysis, aimed at determining whether or not these quantitative variables are spatially continuous across the domain boundaries. In this paper, we present several tools such as cross-to-direct variogram ratios, cross-correlograms, pseudo cross-variograms and lagged scatter plots that are useful for such an analysis and discuss their strengths and weaknesses. The tools are illustrated with applications to synthetic case studies.

1. Introduction

In the analysis of regionalized data, the statistical and spatial distribution of quantitative variables is commonly controlled by categorical variables. For instance, in the modeling of mineral deposits, geological variables such as the metal grades, geotechnical variables such as the rock quality designation (RQD) or the rock mass rating (RMR), or geometallurgical variables such as the metal recovery or crushability and grindability indices (work indices), can depend on categories defined by the rock type or the ore type; likewise, in oil reservoir and aquifer modeling, petrophysical variables such as the porosity or the permeability are typically controlled by lithofacies or hydrofacies (Dubrule, 1993; Yarus and Chambers, 1994; Dowd, 1994, 1997; Sinclair and Blackwell, 2002; Armstrong et al., 2011; Rossi and Deutsch, 2014; Talebi et al., 2019).

The fact that the distribution of the quantitative variables of interest varies according to the rock type or the ore type influences the choice of the most appropriate strategy to be used for modeling these variables and for spatial prediction or simulation. The usual practice consists in partitioning the subsurface into domains (referred to as geological, geotechnical or geometallurgical units) and to separately model the quantitative variables within each domain, i.e., a hierarchical or two-stage approach is adopted, where the quantitative variables are subordinated to the partition into domains. Such an approach commonly assumes the absence of spatial correlation of the quantitative variables across the boundary between two domains and, when so assumed, produces clear-cut discontinuities in the predicted or simulated quantitative variables across a boundary ("hard" geological boundaries) (Duke and Hanna, 2001; Glacken and Snowden, 2001). Some improvements can be considered, for instance, by assigning each target location a probability to belong to each domain (Emery and González, 2007; Séguret, 2013) or by introducing cross-correlations across the domain boundaries (Larrondo et al., 2004; Vargas-Guzmán, 2008; Mery et al., 2017); also, the definition of the domains may not be the same for all the quantitative variables, which allows accounting for different geological controls exerted over these variables (Mery et al., 2017).

An alternative to the above hierarchical approach is a joint approach, in which the domains are considered as covariates for modeling the quantitative variables. For example, for spatial prediction, one can cokrige the quantitative variables together with the domain indicators (Dowd, 1993) or define transition zones in order to account for sampling data of adjacent domains in addition to the data of the target domain (Glacken and Snowden, 2001). For uncertainty quantification, one can develop models to jointly simulate the quantitative and categorical variables, based on combinations of the multi-Gaussian, truncated Gaussian and plurigaussian models (Freulon et al., 1990; Dowd, 1994, 1997; Bahar and Kelkar, 2000; Emery and Silva, 2009; Maleki and Emery, 2015, 2017; Talebi et al., 2017). In such a situation, the interpolation of quantitative variables resulting from cokriging or simulation does not exhibit discontinuities near the domain boundaries,

* Corresponding author.
E-mail address: mohammad.maleki@ucn.cl (M. Maleki).

https://doi.org/10.1016/j.oregeorev.2020.103397
Received 4 January 2019; Received in revised form 7 January 2020; Accepted 9 February 2020
Available online 12 February 2020

thus producing "soft" geological boundaries.

To decide which approach is the most suitable, one can perform a "contact analysis", to determine whether or not the quantitative variables vary continuously across a geological boundary. In particular, one may look at the variation of the mean values as a function of the distance to the boundary, or at the spatial correlation across the boundary (Wilde and Deutsch, 2012; Séguret, 2013; Rossi and Deutsch, 2014; Maleki and Emery, 2015, 2017; Tolosana-Delgado et al., 2016). This exploratory stage is critical in the decision of which strategy (hierarchical or joint modeling) to adopt for spatial prediction or uncertainty quantification.

In this context, the main objective of this paper is to review existing tools and to provide complementary tools that can be used for contact analysis, and to demonstrate the strengths and weaknesses of these tools through synthetic case studies. The outline is the following: Sections 2 and 3 provide details on the synthetic case studies and on the geostatistical model that is used for illustrating the proposed contact analysis tools (Section 4). A discussion and conclusions follow in Sections 5 and 6.

2. Synthetic case studies

Three synthetic case studies were generated, with one quantitative variable (say, a metal grade) and three domains (say, rock type domains). In each case, a ground truth is known over a two-dimensional grid with 2000 nodes along each direction and regular spacing of 1×1. The differences between one case and the other stem from the differences in the grade behavior close to the domain boundaries.

2.1. Case study #1: no geological boundary

In this case, the grade was simulated as the exponential of a stationary Gaussian random field defined over the entire grid, whereas the rock type was simulated as an independent stationary plurigaussian random field with three categories exhibiting regular boundaries (Fig. 1). Accordingly, up to statistical fluctuations, there is no difference in the distribution and spatial behavior of the grade in the three rock type domains and no discontinuity across the domain boundaries.

2.2. Case study #2: hard geological boundaries

Here, three rock type domains were first constructed with a plurigaussian simulation, then an independent lognormal random field was simulated within each domain to represent the metal grade (Fig. 2). Abrupt changes in the distribution and spatial continuity of the grade occur in the rock type boundaries, and grades do not correlate across the boundaries. The mean grades were set to 2.3, 3.0 and 3.8 for domains 1, 2 and 3, whereas the variances were set to 0.4, 0.7 and 1.0, respectively.

2.3. Case study #3: soft geological boundaries

This last case study was constructed in a way similar to case #1, except that the random fields representing the grade and rock type were no longer independent. Specifically, two correlated stationary Gaussian random fields were simulated; the first random field was transformed into a lognormal grade by applying an exponential function, whereas the second random field was truncated in order to yield the rock type (Fig. 3). Here, the rock type boundaries are irregular and there is a spatial ordering between the rock type domains: rock type 2 (medium average grade) separates rock type 1 (low average grade) from rock type 3 (high average grade).

3. Geostatistical modeling

3.1. Notation

Let d be the workspace dimension and $D_1 \ldots D_n$ non-overlapping open subsets of $\mathbb{R}^d$ (i.e., each subset does not contain its boundary) such that the union of their closures is equal to $\mathbb{R}^d$. Also, let J and K be two disjoint subsets of $\{1,\ldots,n\}$, i.e., $J \cap K = \emptyset$ and $J \cup K \subseteq \{1,\ldots,n\}$, and denote by D_J and D_K the associated groups of domains:

$$D_J = \bigcup_{j \in J} D_j \text{ and } D_K = \bigcup_{k \in K} D_k \tag{1}$$

It is of interest to study the behavior of a quantitative variable (metal grade), represented by a random field Z defined in the union of the open domains ($D_1 \cup \ldots \cup D_n$), near the boundary between two domains (D_j and D_k) or, more generally, between two groups of domains (D_J and D_K). Note that the random field Z is left undefined on the domain boundary, in order to avoid any ambiguity in its values in case that it is discontinuous across a domain boundary. Provided that the domains $D_1 \ldots D_n$ are not too irregular, the measure of their boundaries is negligible, so that the random field Z is defined almost everywhere.

Following Séguret (2011, 2013), to ease the analysis of the behavior of Z near the boundary between D_J and D_K, we introduce the "partial grade" $Z_{J,K}$, defined only in the union of these two domains, as:

$$\forall\, \mathbf{x} \in D_J \cup D_K,\ Z_{J,K}(\mathbf{x}) = \begin{cases} Z(\mathbf{x}) & \text{if } \mathbf{x} \in D_J \\ 0 & \text{if } \mathbf{x} \in D_K \end{cases} \tag{2}$$

Likewise, let us introduce the indicator $I_{J,K}$ defined in the union of D_J and D_K as:

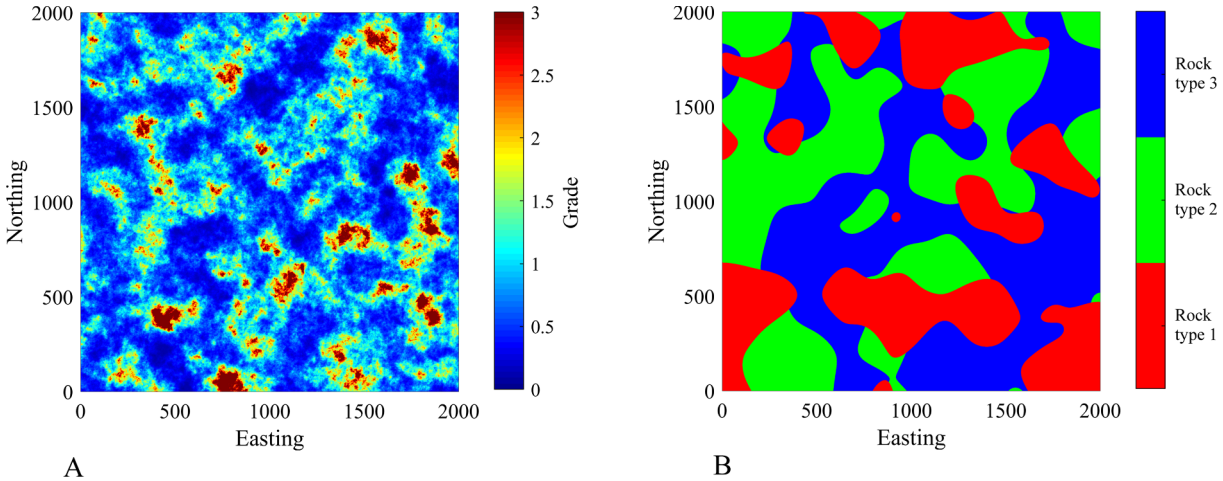

Fig. 1. Simulated lognormal grade (A) and rock type domains (B) for case study #1.

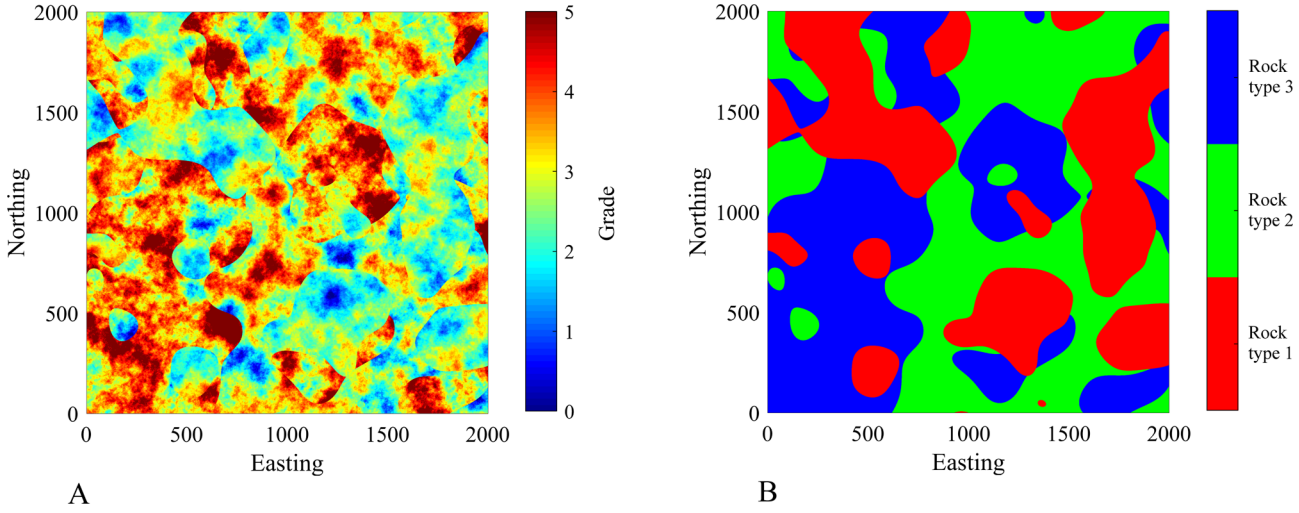

Fig. 2. Simulated piecewise lognormal grade (A) and rock type domains (B) for case study #2.

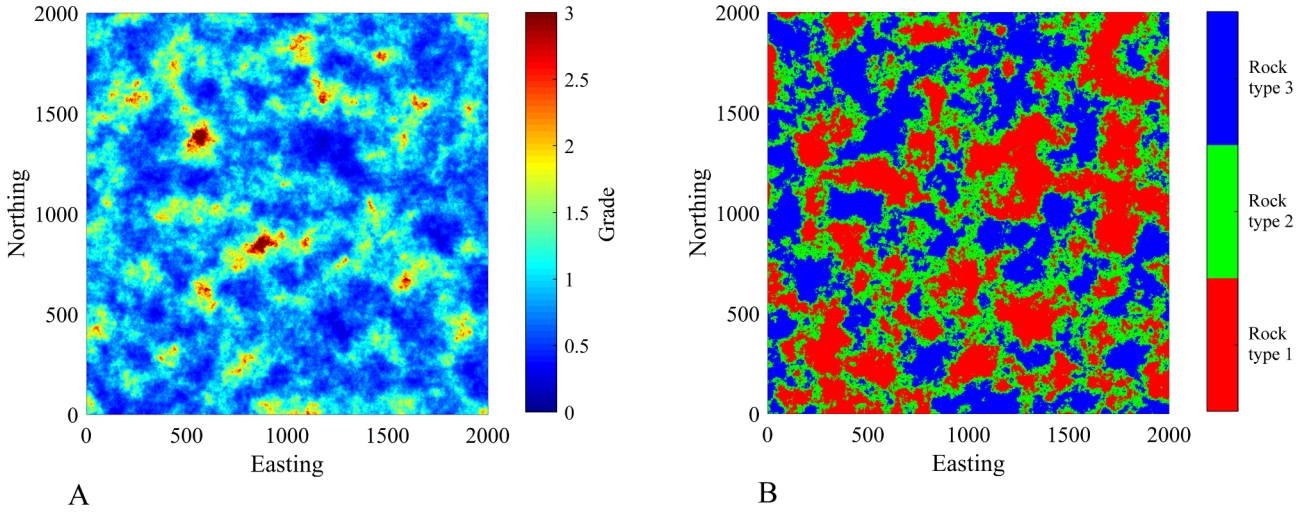

Fig. 3. Simulated lognormal grade (A) and rock type domains (B) for case study #3.

$$\forall\, \mathbf{x} \in D_J \cup D_K,\ I_{J,K}(\mathbf{x}) = \begin{cases} 1 \text{ if } \mathbf{x} \in D_J \\ 0 \text{ if } \mathbf{x} \in D_K \end{cases} \tag{3}$$

When $J \cup K = \{1,\ldots, n\}$, i.e., the closures of D_J and D_K cover the entire space $\mathbb{R}^d$, we may simplify the previous notation and write I_J instead of $I_{J,K}$.

3.2. Various types of geological boundaries

Two different characteristics may be helpful to describe the spatial behavior of a quantitative variable near a geological boundary:

1) the continuity of the variable across the boundary;
2) the variations of its mean value as a function of the distance to the boundary.

The first characteristics defines whether the boundary is *hard*, if the variable exhibits a clear-cut discontinuity, or *soft*, if it remains continuous across the boundary (Duke and Hanna, 2001; Glacken and Snowden, 2001). In contrast, the second characteristics defines the presence of a *border effect* or *edge effect*, if the mean value varies depending on the distance to the boundary, or the absence of it if, on each side of the boundary, the mean value remains constant, irrespective of the distance to the boundary (Rivoirard, 1993, 1994; Séguret, 2013). Both characteristics are not exclusive and one can find hard boundaries with and without edge effects (see Discussion section hereafter).

3.3. Piecewise random field modeling

We assume that there exists a set of n random fields $Z_1,\ldots, Z_n$ defined in $\mathbb{R}^d$ such that, within each open domain D_j, $j \in \{1,\ldots, n\}$, Z coincides with Z_j:

$$\forall\, \mathbf{x} \in D_1 \cup \ldots \cup D_n,\ Z(\mathbf{x}) = \sum_{j=1}^{n} Z_j(\mathbf{x})\, I_j(\mathbf{x}) \tag{4}$$

with I_j the indicator of domain D_j (Eq. (3)). One therefore obtains a piecewise model defined in the union of the domains under study and undefined on the domain boundaries. Such a model combines two sources of randomness that account for geological uncertainty: on the one hand, the domain indicators $I_1,\ldots, I_n$ (binary random fields); on the other hand, the continuous random fields $Z_1,\ldots, Z_n$.

Let us now assume that $(I_1,\ldots, I_n, Z_1,\ldots, Z_n)$ are jointly stationary, i.e., their finite-dimensional distributions (in particular, their means, variances, direct and cross-covariance functions and variograms) are invariant by a translation in space. As a consequence, the piecewise random field Z (Eq. (4)) is also stationary, as a combination of stationary random fields.

The assumption of stationarity is useful to ensure that the global

Table 1
Prior and posterior (conditional) mean values of $Z(\mathbf{x})$ ($\mathbb{E}$ indicates the expectation operator). All these mean values are independent of $\mathbf{x}$ owing to the stationarity assumption.

Random variable	Conditioning information	Expected value	Mathematical definition
$Z(\mathbf{x})$	None	m	$\mathbb{E}\{Z(\mathbf{x})\}$
$Z(\mathbf{x})$	$\mathbf{x} \in D_J$	m_J	$\mathbb{E}\{Z(\mathbf{x})\|\mathbf{x} \in D_J\}$
$Z(\mathbf{x})$	$\mathbf{x} \in D_J$, $\mathbf{x} + \mathbf{h} \notin D_J$	$m_J(\mathbf{h})$	$\mathbb{E}\{Z(\mathbf{x})\|\mathbf{x} \in D_J, \mathbf{x} + \mathbf{h} \notin D_J\}$
$Z(\mathbf{x})$	$\mathbf{x} \in D_J$, $\mathbf{x} + \mathbf{h} \in D_K$	$m_{J,K}(\mathbf{h})$	$\mathbb{E}\{Z(\mathbf{x})\|\mathbf{x} \in D_J, \mathbf{x} + \mathbf{h} \in D_K\}$

statistics are invariant under translation and can be estimated by the associated experimental statistics calculated from sampling information on the quantitative variable and domains. The pertinence of this assumption is discussed further in Section 5.3.

Apart from global statistics, one can also define conditional statistics on Z that will be helpful to describe the nature of the geological boundaries. Some examples are indicated in Table 1. The conditioning information modifies the prior statistics, so that the conditional mean values defined in Table 1 are likely to be different from the prior mean (overall average of Z over the entire space).

One can now formalize the previous concepts related to the nature of a geological boundary:

- If Z_j and Z_k are the same random field and are continuous (without nugget effect), then no discontinuity is observed across the boundary between D_j and D_k, which turns out to be a soft boundary. In contrast, if Z_j and Z_k are two different random fields, then the boundary between D_j and D_k will be hard.
- If Z_j is independent of I_j, then there is no edge effect within D_j. Indeed, the expected value at a given location $\mathbf{x}$ within D_j does not depend on whether or not another location $\mathbf{x} + \mathbf{h}$ lies outside D_j, i.e., it does not depend on whether $\mathbf{x}$ is close to the boundary of D_j or not:

$$\begin{aligned} m_j(\mathbf{h}) &= \mathbb{E}\{Z(\mathbf{x})|\mathbf{x} \in D_j, \mathbf{x}+\mathbf{h} \notin D_j\} \\ &= \mathbb{E}\{Z_j(\mathbf{x})|I_j(\mathbf{x}) = 1, I_j(\mathbf{x}+\mathbf{h}) = 0\} \\ &= \mathbb{E}\{Z_j(\mathbf{x})\} = m_j \end{aligned} \tag{5}$$

On the contrary, if Z_j and I_j are dependent, then the conditional mean value $m_j(\mathbf{h})$ may differ from m_j and one may therefore observe an edge effect within D_j. The magnitude of such an edge effect can be direction-dependent if the cross-covariance between Z_j and I_j is anisotropic; it can also not be the same in one direction and in the opposite direction if the cross-covariance between Z_j and I_j is not an even function.

In summary, the proposed piecewise random field is suited to the modeling of both soft and hard boundaries, as well as to the modeling of edge effects or the absence of them. The three synthetic case studies presented in Section 2 are particular representations of this piecewise model.

4. Tools for contact analysis

4.1. First tool: mean grade variation

The first tool proposed for contact analysis is the conditional mean $m_J(\mathbf{h})$ defined in Table 1, which represents the expected grade at a location $\mathbf{x}$ given that $\mathbf{x}$ belongs to D_J and $\mathbf{x} + \mathbf{h}$ does not belong to this domain. Based on Rivoirard (1993, 1994) and on an assumption of spatial symmetry, Séguret (2013) proved that this conditional mean coincides with the following cross-to-direct variogram ratio:

$$\forall\, \mathbf{h} \in \mathbb{R}^d,\ m_J(\mathbf{h}) = \frac{\gamma_{Z_J,\bar{J}\, I_J}(\mathbf{h})}{\gamma_{I_J}(\mathbf{h})} \tag{6}$$

where $\bar{J}$ denotes the complement of J in $\{1,\ldots, n\}$: $J \cap \bar{J} = \varnothing$ and $J \cup \bar{J} = \{1, \ldots, n\}$. The numerator in (6) is the cross-variogram between the partial grade $Z_{J,J}$ and the indicator I_J, whereas the denominator is the direct variogram of I_J. The ratio depends only on the separation vector $(\mathbf{h})$ because of the stationarity assumption. It indicates how the local mean grade in D_J varies in the vicinity of (small $|\mathbf{h}|$) or far from (large $|\mathbf{h}|$) the domain boundary.

One can get more detailed information on the mean grade variation near a domain boundary by considering the conditional mean $m_{J,K}(\mathbf{h})$, as defined in Table 1, which indicates how the local mean grade in D_J varies in the vicinity of (small $|\mathbf{h}|$) or far from (large $|\mathbf{h}|$) the boundary with D_K. It can be shown (Appendix A) that this conditional mean also coincides with a partial grade-indicator cross-to-direct variogram ratio:

$$\forall\, \mathbf{h} \in \mathbb{R}^d,\ m_{J,K}(\mathbf{h}) = \frac{\gamma_{Z_{J,K}\, I_{J,K}}(\mathbf{h})}{\gamma_{I_{J,K}}(\mathbf{h})} \tag{7}$$

This tool actually yields the same information as the contact plots presented by Wilde and Deutsch (2012), Rossi and Deutsch (2014), Maleki and Emery (2015) or Mery et al. (2017). Analogous tools can be designed in order to characterize the gradient of grade across a geological boundary (Appendix B).

As an illustration, let us apply the cross-to-direct variogram ratios to the three synthetic case studies defined in Section 2 (Fig. 4). For the first case study, the experimental estimate of $m_1(\mathbf{h})$ show that the local mean grade in D_1 does not vary if one gets closer to the domain boundary. However, the estimates of $m_{1,2}(\mathbf{h})$ and $m_{1,3}(\mathbf{h})$ suggest the presence of an edge effect within D_1, with the local mean grade in D_1 slightly increasing if one gets closer to the boundary with D_2 and slightly decreasing if one gets closer to the boundary with D_3 (Fig. 4A). In the present case, such an edge effect is the result of statistical fluctuations, insofar as the grade is, by construction, independent of the domains. Comparing the estimates of $m_{1,2}(\mathbf{h})$ and $m_{2,1}(\mathbf{h})$ near the origin ($|\mathbf{h}| \to 0$) (Fig. 4A, 4B) reveals the same local mean value on both sides of the boundary between D_1 and D_2. The same actually happens with the estimates of $m_{j,k}(\mathbf{h})$ and $m_{k,j}(\mathbf{h})$ for any pair (j,k) of indices in $\{1,2,3\}$, indicating that the mean grade is continuous across the domain boundaries, in agreement with the construction of the case study (the grade is represented by a single continuous random field defined over the entire space).

The continuity of the mean grade across the domain boundaries is also observed in the third case study (Fig. 4G-4I) corresponding to a soft boundary model, where the estimates of $m_{j,k}(\mathbf{h})$ and $m_{k,j}(\mathbf{h})$ tend to be the same as $|\mathbf{h}| \to 0$. Here, these functions exhibit greater variations at short scale (small values of $|\mathbf{h}|$) than in the first case study, i.e., the variations of mean grade in the vicinity of the domain boundaries are more pronounced. This can be explained because the domains are correlated with the grade, with D_1 having the lowest average grade and D_3 having the highest one, which implies the presence of edge effects. Note that the estimate of $m_2(\mathbf{h})$ does not reflect any variation in the local mean grade of D_2 in the vicinity of the boundary (Fig. 4H) because the grade increase in the vicinity of D_3 is compensated by the grade decrease in the vicinity of D_1. In this respect, $m_j(\mathbf{h})$ conveys less information than $m_{j,k}(\mathbf{h})$ on the grade behavior near the domain boundaries.

As for the second case study (Fig. 4D-4F), the existence of hard boundaries is reflected by the fact that the estimates of $m_{j,k}(\mathbf{h})$ and $m_{k,j}(\mathbf{h})$ do not tend to the same value as $|\mathbf{h}| \to 0$: crossing a domain

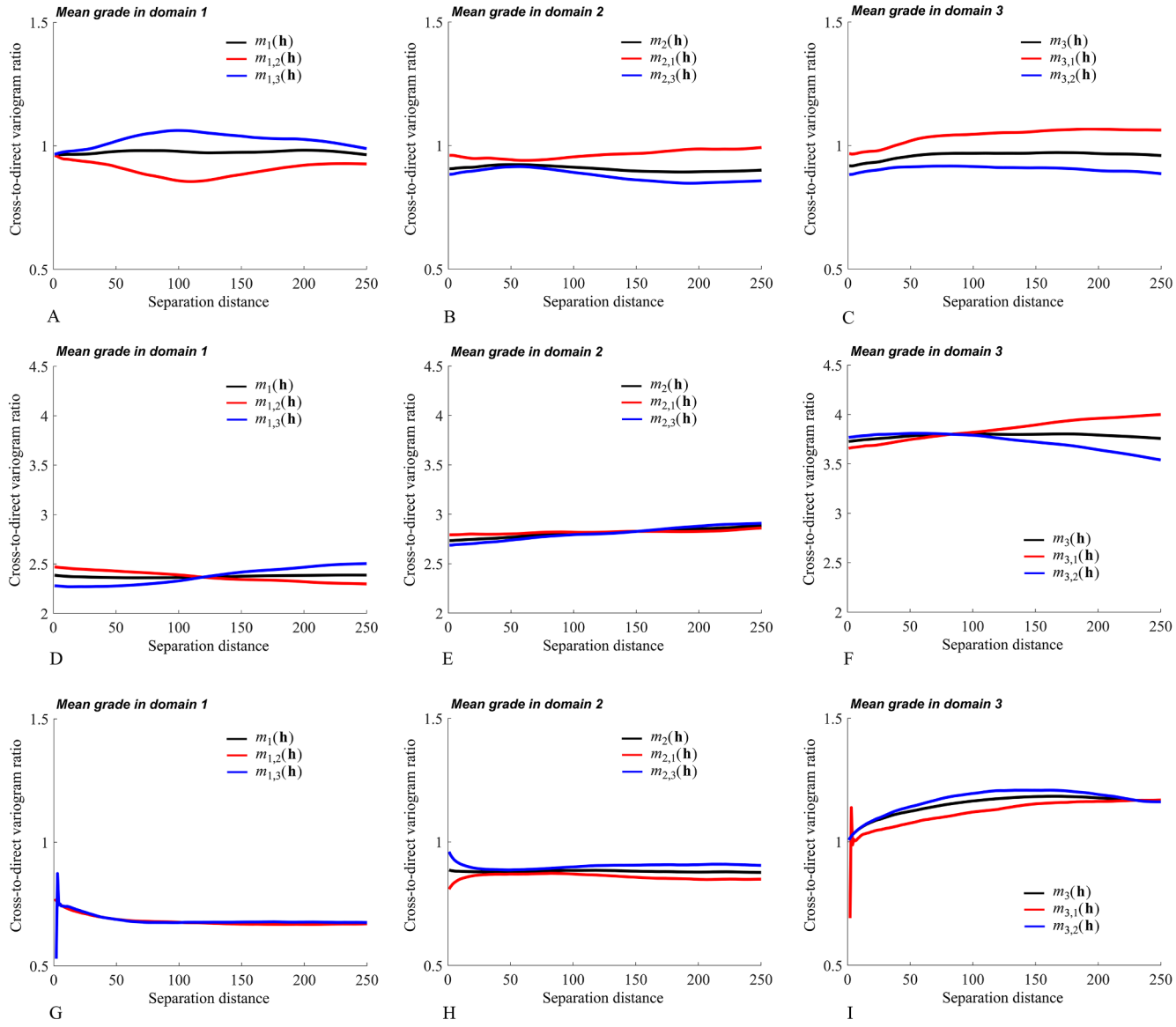

Fig. 4. Estimates of $m_j(\mathbf{h})$ and $m_{j,k}(\mathbf{h})$ as functions of $|\mathbf{h}|$ for synthetic case studies #1 (A-C), #2 (D-F) and #3 (G-I), showing the variations in the mean grade in the vicinity of or far from the domain boundaries.

boundary implies a discontinuity in the local mean grade and, *a fortiori*, in the grade itself. The curves in Fig. 4D-4F also suggest the presence of edge effects, which are actually produced by statistical fluctuations as they have not been imposed by the construction of the case study.

4.2. Second tool: grade correlation across boundaries

The analysis of mean grade variations can be complemented by the calculation of the cross-correlation between the grades in different domains. In this line, Larrondo et al. (2004), Vargas-Guzmán (2008) and Mery et al. (2017) propose the use of cross-covariance functions for grade prediction or simulation accounting for sampling data on both sides of a geological boundary.

Instead of the cross-covariance, following Maleki and Emery (2015, 2017), we suggest the use of the cross-correlation function (cross-correlogram). Under the stationarity assumption, this function provides a normalized measure (between -1 and 1) of the linear dependence relationship between the grades within different domains, as a function of the separation vector:

$$\forall\, \mathbf{h} \in \mathbb{R}^d,\ \rho_{J,K}(\mathbf{h}) = corr\{Z(\mathbf{x}), Z(\mathbf{x}+\mathbf{h}) | \mathbf{x} \in D_J,\ \mathbf{x}+\mathbf{h} \in D_K\} \tag{8}$$

In the case of no boundary or of a soft boundary (synthetic case studies #1 and #3), the experimental cross-correlation is high at short distances, ideally tending to 1 as $|\mathbf{h}|$ tends to 0, and decreases at increasing distances (Fig. 5A, 5C). On the contrary, in the presence of hard boundaries without edge effects (synthetic case study #2), the experimental cross-correlation is weak (close to zero) at short distances (Fig. 5B).

4.3. Third tool: grade contrasts across boundaries

A third tool that can be used for contact analysis is the mean squared difference between the grades observed in D_J and D_K, which reflects the grade contrast across the boundary between both domains:

$$\forall\, \mathbf{h} \in \mathbb{R}^d,\ 2\gamma_{J,K}(\mathbf{h}) = \mathbb{E}\{[Z(\mathbf{x}) - Z(\mathbf{x}+\mathbf{h})]^2 | \mathbf{x} \in D_J,\ \mathbf{x}+\mathbf{h} \in D_K\} \tag{9}$$

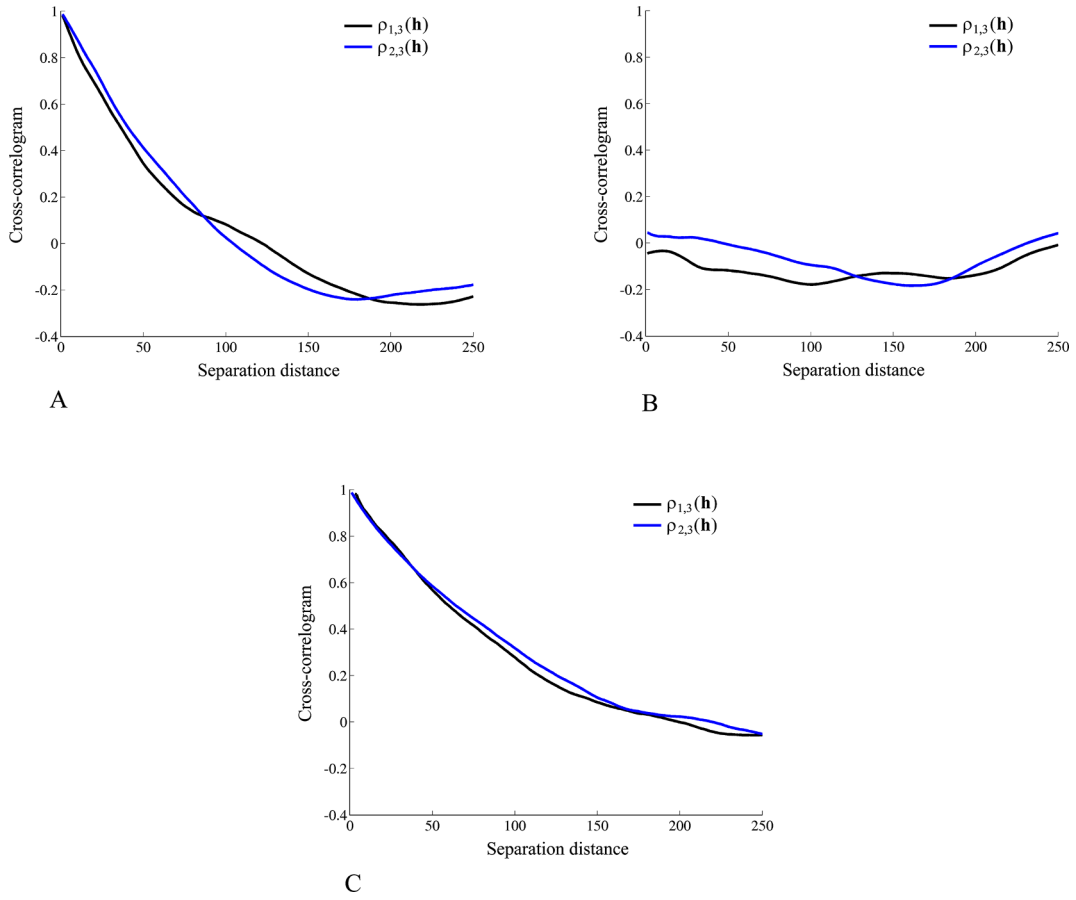

Fig. 5. Estimates of $\rho_{j,3}(\mathbf{h})$ as a function of $|\mathbf{h}|$ for synthetic case studies #1 (A), #2 (B) and #3 (C), showing the grade correlations across the boundaries of domain D_3.

This tool depends only on $\mathbf{h}$ due to the joint stationarity of Z_J and Z_K. It corresponds to the pseudo cross-variogram introduced by Clark et al. (1989), applied here to contact analysis purposes, as suggested by Ortiz and Emery (2006).

For illustration, this tool is applied to the three synthetic case studies (Fig. 6). In the first case study, the experimental pseudo cross-variogram tends to 0 at short distances, reflecting that the grade is continuous across the boundaries. In the second case study, it tends to a positive value, indicating a discontinuity in the grade (hard geological boundaries). In the third case study (soft boundaries), because the grade is continuous across the boundary, one expects an experimental pseudo cross-variogram tending to 0 at short distances, but this does not happen so clearly in the case of the boundary between D_1 and D_3 (Fig. 6C). This is explained because these two domains have little direct contact (D_1 and D_3 tend to be separated by D_2), which makes the experimental statistics unrobust, and because of the presence of a strong edge effect (D_1 exhibits low grades whereas D_3 exhibits high grades, according to the construction of the case study), making the local mean grades in both domains being different as soon as they are calculated at a non-zero distance to the boundary.

4.4. Fourth tool: lagged scatter plots

The last tool presented in this research is the lagged scatter plot or $\mathbf{h}$-scattergram. So far, this tool is mainly used for data cleaning and detection of mixtures of populations in exploratory analyses and for validating bivariate distribution models (Rivoirard, 1994; Goovaerts, 1997; Emery, 2005; Chilès and Delfiner, 2012). In the context of contact analysis, the lagged scatter plot consists in comparing the grades at two adjacent sampling locations separated by a given vector (up to some tolerances on the vector norm and/or direction), subject to the fact that both locations belong to different domains.

Examples of such plots for the three synthetic case studies under consideration are presented in Fig. 7 for the contact between D_1 and D_3; the chosen separation vector is oriented along the abscissa axis with a norm of 10 units. The plots allow a comparison of the mean grades near the boundary between D_1 and D_3 and, at the same time, an analysis of the correlation across this boundary. In the absence of boundary (case study #1), the mean grade does not change (the gravity center of the point cloud lies over the diagonal line) and the correlation is high (0.89) (Fig. 7A). The opposite happens in the case of hard boundaries without edge effects (case study #2): one observes a change in the mean grade and a low correlation (Fig. 7B). The case study #3 with soft boundaries exhibits a high correlation (0.91) across the boundaries, with a slight change in the mean grade (Fig. 7C), again due to the strong edge effect and the fact that the lagged scatter plot is calculated for a non-zero distance.

5. Discussion

5.1. Strengths and weaknesses of the proposed tools

The four presented tools convey different levels of information on the nature of a geological boundary. The cross-to-direct variogram ratio provides information on the mean grade, but not on the grade correlation across the boundary, whereas the reverse happens for the cross-correlogram. One of these two tools alone may be insufficient to detect the true nature of the boundary. For instance, one can imagine a hard boundary for which the grades measured on both sides are independent but such that the mean grade does not change, giving a false impression

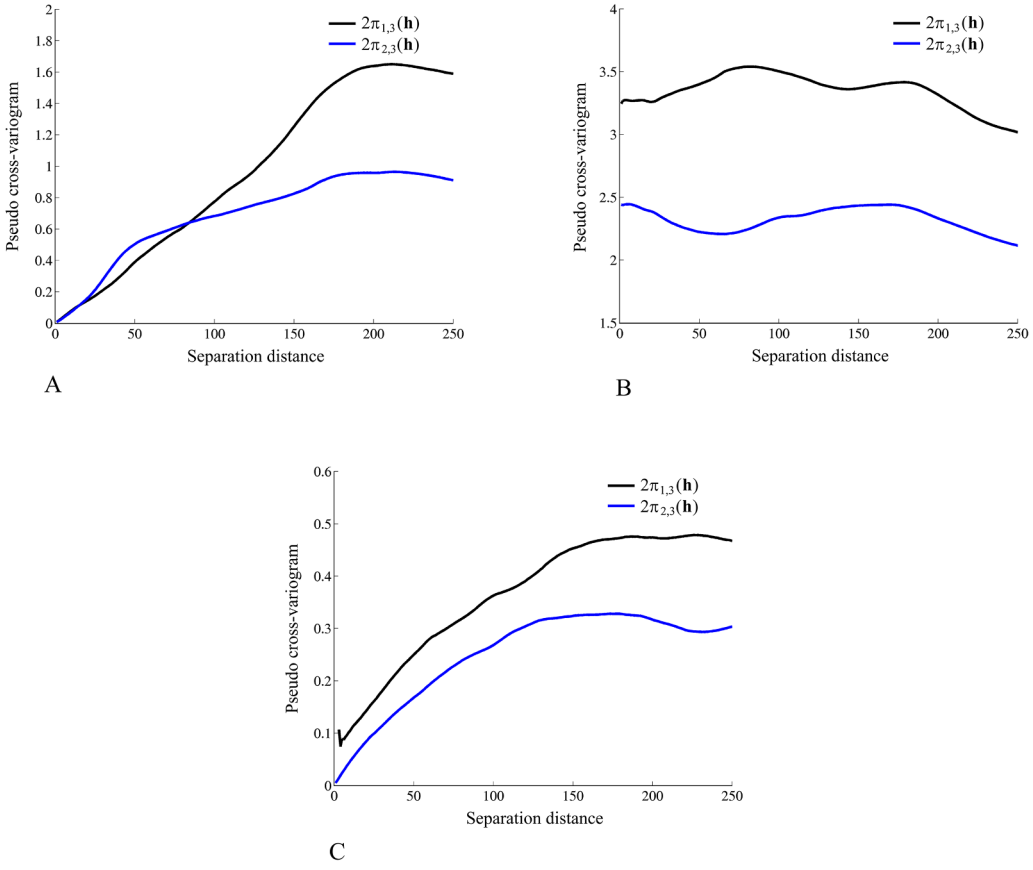

Fig. 6. Estimates of $2\pi_{j,3}(\mathbf{h})$ as a function of $|\mathbf{h}|$ for synthetic case studies #1 (A), #2 (B) and #3 (C), showing the grade contrasts across the boundaries of domain D_3.

of continuity if one looks at the cross-to-direct variogram ratios. Another example is given by a hard boundary, on both sides of which the mean grades are significantly different but correlated across the boundary (e.g., if the grade locally increases on one side, it tends to increase on the other side, due to alteration, impregnation or diffusion processes). In this case, the cross-correlogram would indicate a spatial correlation of the grade across the boundary; however, such a correlation would not be the manifestation of a continuous behavior of the grade (soft boundary), but rather of an edge effect.

In contrast, by calculating the mean squared difference between the grades measured in two domains, the pseudo cross-variogram incorporates information on both the mean variations and the correlation across the domain boundaries:

$$\begin{aligned} 2\pi_{J,K}(\mathbf{h}) &= var\{Z(\mathbf{x}) - Z(\mathbf{x}+\mathbf{h}) | \mathbf{x} \in D_J, \mathbf{x}+\mathbf{h} \in D_K\} \\ &+ \mathbb{E}^2\{Z(\mathbf{x}) - Z(\mathbf{x}+\mathbf{h}) | \mathbf{x} \in D_J, \mathbf{x}+\mathbf{h} \in D_K\} \\ &= \text{var}\{Z_J(\mathbf{x}) | \mathbf{x} \in D_J, \mathbf{x}+\mathbf{h} \in D_K\} + \text{var}\{Z_K(\mathbf{x}+\mathbf{h}) | \mathbf{x} \in D_J, \mathbf{x}+\mathbf{h} \in D_K\} \\ &- 2\underbrace{\text{cov}\{Z_J(\mathbf{x}), Z_K(\mathbf{x}+\mathbf{h}) | \mathbf{x} \in D_J, \mathbf{x}+\mathbf{h} \in D_K\}}_{\text{cross - covariance}} \\ &+ \underbrace{\text{E}^2[Z_J(\mathbf{x}) - Z_K(\mathbf{x}+\mathbf{h}) | \mathbf{x} \in D_J, \mathbf{x}+\mathbf{h} \in D_K]}_{\text{mean variation (gradient)}} \end{aligned} \quad (10)$$

A drawback of the pseudo cross-variogram is its lack of standardization, unlike the cross-correlogram that is bounded between -1 and 1.

Likewise, as seen in the previous case studies, the lagged scatter plot allows appraising the differences in local mean grade and, at the same time, the correlation across a geological boundary. The experimental cross-correlogram and pseudo-cross variogram for a given separation vector $\mathbf{h}$ actually correspond to the correlation coefficient and to the moment of inertia of the lagged scatter plot for this separation vector, respectively.

It should also be mentioned that the cross-to-direct variogram ratio is an even function and, unlike the other three tools, does not provide information on oriented grade transitions, a feature observed in cyclic depositional environments (Maleki et al., 2017; Le Blévec et al., 2018). An assumption of symmetry in the joint spatial distribution of the grade and domain indicators has to be made to give an interpretation to the variogram ratio, or alternative tools based on cross-covariances instead of cross-variograms have to be designed (Appendix C).

All in all, the authors advocate the use of the lagged scatter plot, because it displays the values of all the data pairs situated across the boundary, and not only average statistics calculated over these pairs; in particular, this allows the identification and cleaning of outlying data. However, one can argue that the experimental variogram ratios, correlograms and pseudo cross-variograms display information for several separation vectors simultaneously, and therefore provide richer information than a single lagged scatter plot. For small separation distances ($|\mathbf{h}|$ close to 0), the conveyed information reflects the grade behavior close to the domain boundaries, insofar as the calculations involve two nearby locations $\mathbf{x}$ and $\mathbf{x}+\mathbf{h}$ situated in different domains. However, for large separation distances, it is less evident that the experimental variogram ratios, cross-correlograms and pseudo cross-variograms describe the grade behavior within the inner core of each domain, because their calculations involve locations situated at distances that can vary between 0 and $|\mathbf{h}|$ from the domain boundary (Fig. 8). In practice, this makes these tools more difficult to interpret at large distances.

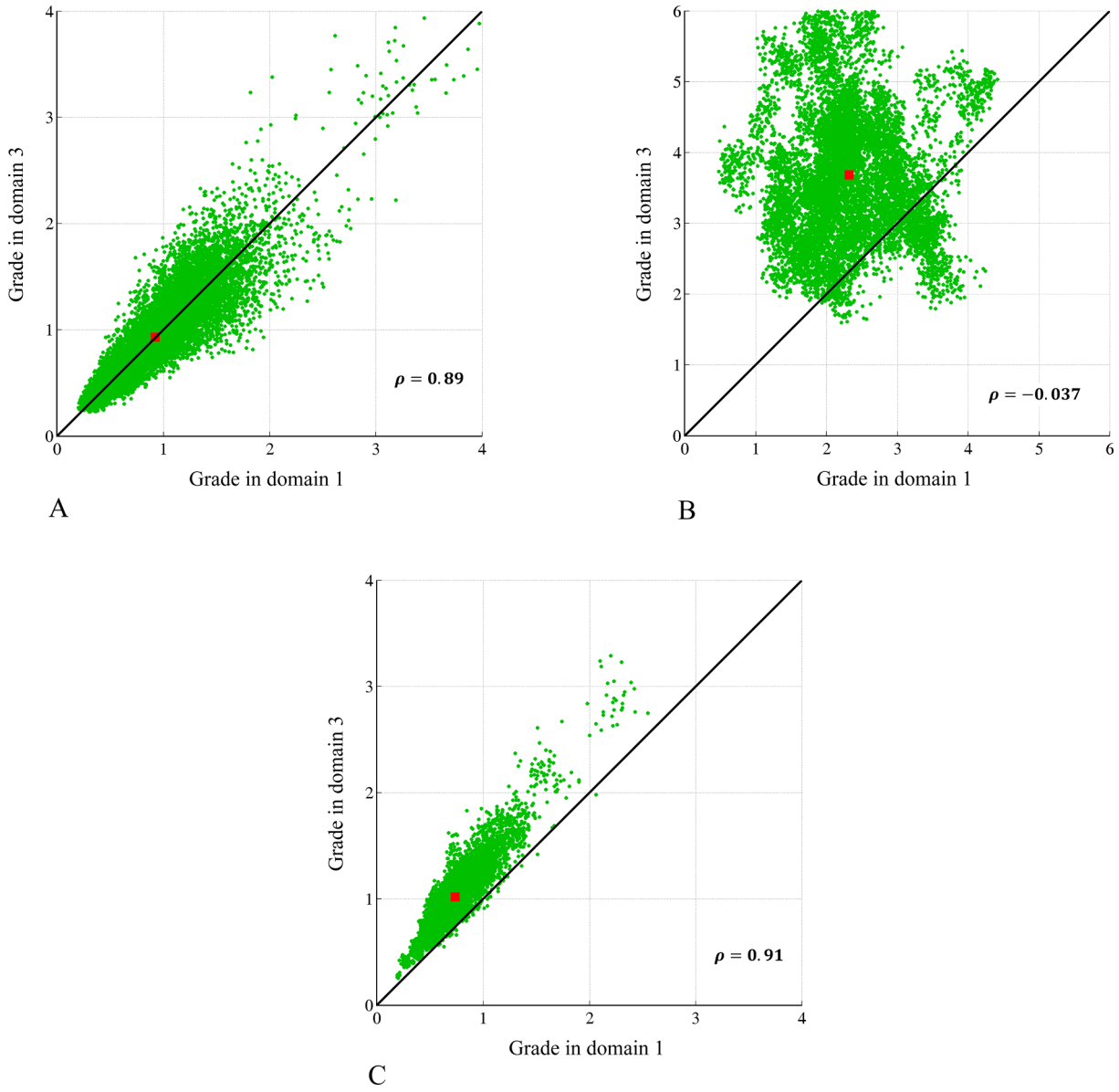

Fig. 7. Lagged scatter plots between the grades in domains D_1 and D_3, associated with a separation distance of 10 units, for synthetic case studies #1 (A), #2 (B) and #3 (C). The red squares indicate the gravity centers of the scatter plots. (For interpretation of the references to colour in this figure legend, the reader is referred to the web version of this article.)

5.2. Nature of geological boundaries

Practitioners may distinguish more than two (hard/soft) types of geological boundaries, introducing concepts such as *semi-soft boundary* if the contact plot of the mean grade as a function of the distance to the boundary shows a continuous transition on both sides at a short scale, *semi-hard boundary* if the transition on both sides goes with a discontinuity, or *one-way transparent boundary* if the transition is observed only on one side (Fig. 9C, 9E, 9F) (Glacken and Snowden, 2001). Actually, all these types of boundaries can be classified into either hard or soft if one adopts the following definition:

(1) A soft boundary is characterized by a continuous grade variation across a domain boundary. The underlying geostatistical model is that of a single random field defined on both sides of the boundary. Such a grade random field can be independent of the domain indicator (Fig. 9A), meaning no influence of the domain on the grade as if there were no boundary, or it can be correlated with it, which is likely to modify the statistics of the grade in the vicinity of the boundary and imply the presence of an edge effect, as seen in the third synthetic case study. From a mathematical point of view, this is explained because the grade distribution conditioned to the domain indicator differs from the prior (non-conditional) grade distribution; in particular, the conditional mean grades $m_J(\mathbf{h})$ or $m_{J,K}(\mathbf{h})$ defined in Table 1 are likely to vary with $\mathbf{h}$. The spatial correlation between grade and indicator can be of long (Fig. 9B) or short (Fig. 9C) range.

(2) A hard boundary is characterized by a discontinuous variation of grade across a domain boundary. The underlying geostatistical model is that of two different random fields, each one associated with one side of the boundary. These two random fields and the domain indicator can be mutually independent (Fig. 9D) (no edge effect) or cross-correlated (presence of an edge effect); in turn, the spatial cross-correlation functions can be symmetric (Fig. 9E) or asymmetric (Fig. 9F).

Diagnosing whether a geological boundary is hard or soft is therefore essential to decide how many different random fields should be

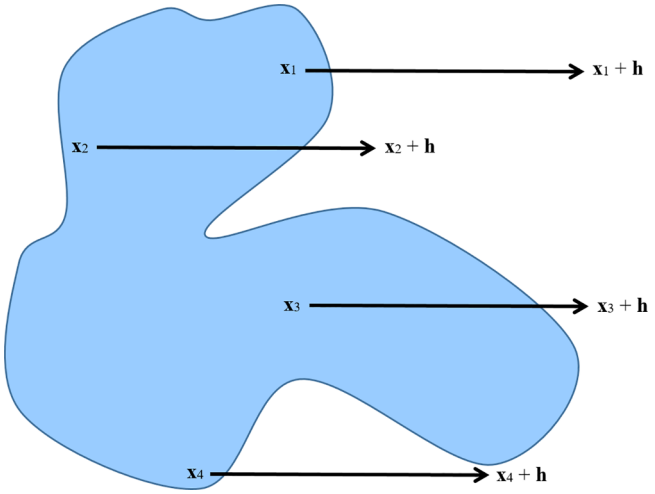

Fig. 8. Examples of pairs of locations situated on both sides of a domain boundary.

used to represent the spatial variations of the grade: a single random field is needed in domains with soft boundaries, whereas as many random fields as domains are needed in case of hard boundaries. In the presence of edge effects, this/these random field(s) may be cross-correlated with the domain indicators, which can be diagnosed at a subsequent stage by examining the direct and cross-covariances or variograms of the grade and domain indicators. Such cross-correlations between grade and domain indicators, if they exist, can be used for spatial prediction and simulation. An example of diagnosis and subsequent modeling, involving both hard and soft boundaries, aimed at simulating the copper grade in a porphyry copper deposit, is presented in Emery and Maleki (2019).

Arguably, from a practical point of view, the distinction between a soft (Fig. 9B) or a hard boundary (Fig. 9E) based on a limited number of sampling data may be unclear and left to the interpretation of the geologist/geostatistician, mainly because the grade can exhibit a nugget effect or short-scale variability, because of the presence of edge effects and/or because of the sampling mesh that prevents calculating contact plots for very small distances to the boundary. As an illustration, the lagged scatter plot in the third case study (Fig. 7C) gives the impression of a discontinuity in the local mean grade across the boundary between D_1 and D_3, hence a hard boundary, due to the presence of a strong edge effect in both domains that makes paired data separated 10 units having significantly different mean grades. The recommendation is therefore not to focus on a single tool for contact analysis, but to jointly examine the mean grade variations, grade correlation, grade contrasts and lagged scatter plots in order to get an accurate interpretation of the nature of a domain boundary (Table 2).

5.3. Back to the assumption of stationarity

A last point for discussion concerns the assumption of stationarity. Observing that the mean grade locally varies in the vicinity of a domain boundary is not incompatible with an assumption of stationarity. Indeed, one has to distinguish between the *prior* distribution of the random field under study (distribution prior to the knowledge of any data on the random field) and its *posterior* distribution (conditioned to sampling information). In particular, if there exists a spatial dependence between the grade and the domain indicators, some domains are likely to exhibit higher grades than others (Fig. 9B, 9C), a situation that occurs in the third synthetic case study with soft boundaries, although, by construction, the prior distribution of the grade in this case study is stationary. An extreme situation, similar to this third case study, would

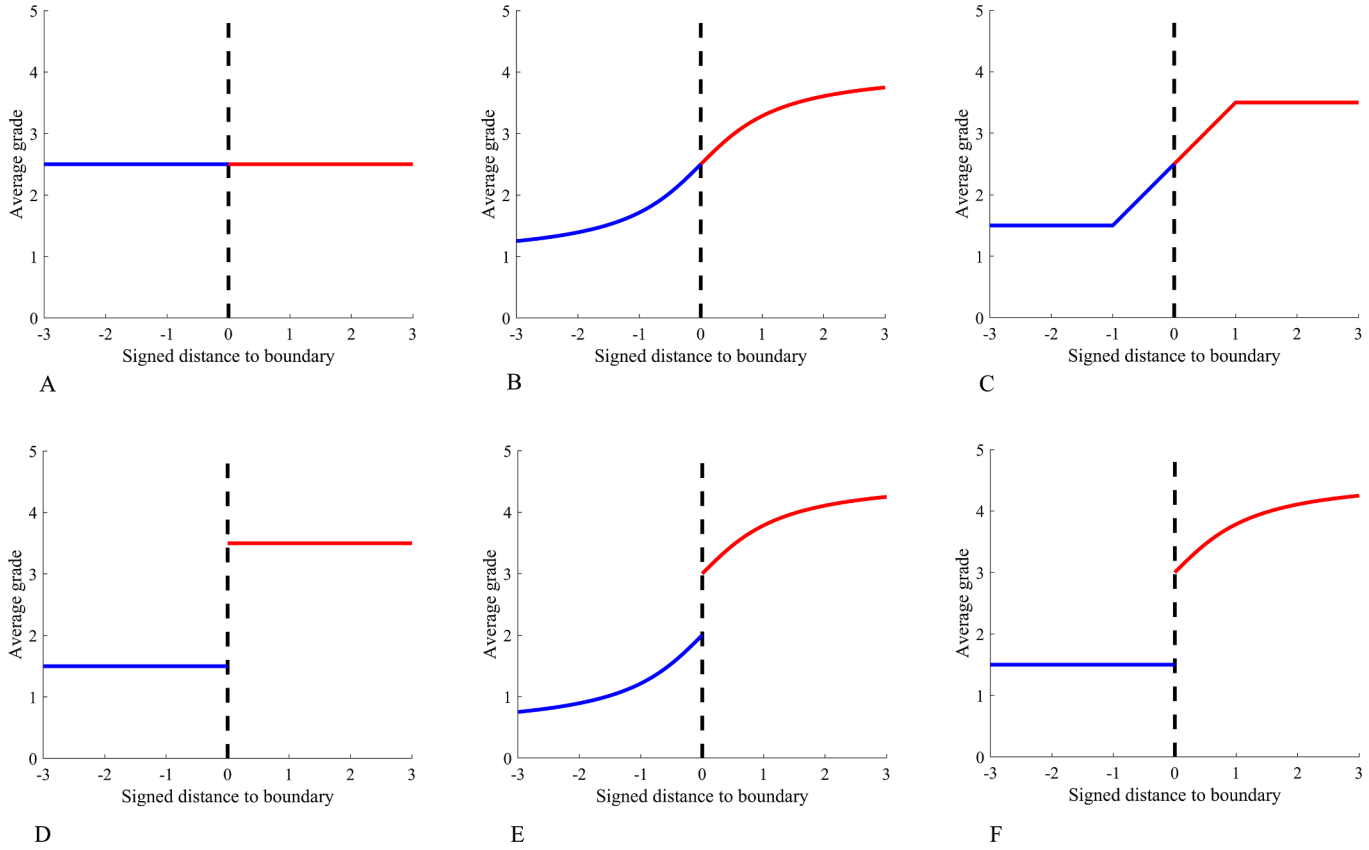

Fig. 9. Examples of contact plots showing the mean grade as a signed function of the distance to the boundary, for soft (A, B, C) and hard (D, E, F) boundaries.

Table 2
Summary of tools for contact analysis.

Tool	Observation	Diagnostic
Cross-to-direct variogram ratio	$m_{J,K}(\mathbf{h})$ and $m_{K,J}(\mathbf{h})$ tend to the same value as $\|\mathbf{h}\|$ tends to 0	Soft boundary, or hard boundary with the same mean value on both sides
	$m_{J,K}(\mathbf{h})$ and $m_{K,J}(\mathbf{h})$ do not tend to the same value as $\|\mathbf{h}\|$ tends to 0	Hard boundary
Cross-correlogram	$\rho_{J,K}(\mathbf{h})$ does not tend to 1 as $\|\mathbf{h}\|$ tends to 0	Hard boundary
	$\rho_{J,K}(\mathbf{h})$ tends to 1 as $\|\mathbf{h}\|$ tends to 0	Soft boundary, or hard boundary with strong correlation across the boundary
Pseudo cross-variogram	$\pi_{J,K}(\mathbf{h})$ tends to 0 as $\|\mathbf{h}\|$ tends to 0	Soft boundary
	$\pi_{J,K}(\mathbf{h})$ does not tend to 0 as $\|\mathbf{h}\|$ tends to 0	Hard boundary
Lagged scatterplot	Scatter plot concentrated along the diagonal line as $\|\mathbf{h}\|$ tends to 0	Soft boundary
	Scatter plot not concentrated along the diagonal line as $\|\mathbf{h}\|$ tends to 0	Hard boundary

be the case of a stationary grade and domains defined by grade shells, which could give a wrong impression of non-stationarity in the first- and also in the second-order moments (Emery and Ortiz, 2005).

In summary, spatial variations in the mean grade near the domain boundaries (edge effects) are compatible with the stationary piecewise model defined in Eq. (4). The edge effects can be the manifestation of a correlation between the grade and the domain indicators. The formalization of such edge effects can rely on the concept of mean grade conditioned to sampling information (Emery and Robles, 2009).

Moreover, for exploratory analysis, one can, without further inconvenience, weaken the strict stationarity assumption to second-order stationarity (i.e., stationarity of the first- and second-order moments only) or, by restricting the analysis to small separation distances, quasi-stationarity (stationarity within a local neighborhood). The development of models that do not rely on the assumption of stationarity for the grade and/or the domain indicators (Patel et al., 1996; Larrondo and Deutsch, 2005; Xu and Dowd, 2009) is of course feasible to describe complex grade behaviors in the vicinity of domain boundaries, at the price of a higher sophistication.

6. Conclusions

A preliminary stage in the modeling of mineral deposits is the identification of geological, geotechnical and geometallurgical domains such that the quantitative variables of interest (metal grades, rock mass rating, metal recoveries, work indices, etc.) behave homogeneously within each domain and differently in different domains. Contact analysis is essential to diagnose the nature of the geological boundary between two domains with respect to a quantitative variable. Essentially, one can distinguish between hard and soft boundaries, depending on whether the variable exhibits a clear-cut discontinuity or not across a geological boundary.

To perform such a contact analysis, four geostatistical tools that can be easily inferred from sampling data have been presented, which are aimed at examining the variations in the mean value (cross-to-direct variogram ratios), the existence of a spatial correlation across a boundary (cross-correlograms), or both features (pseudo cross-variograms and lagged scatter plots). The latter tool is straightforward to interpret, as shown in the synthetic case studies, whereas the three former are more difficult to interpret at large separation distances. The joint analysis of these four tools is nevertheless recommended in order to avoid mistaking the diagnosis in complex situations, e.g., a hard boundary with edge effects, for which one observes variations in the mean values and/or a correlation of the grade across the boundary.

A hard boundary should be modeled by considering two different random fields to represent the grade on each side of the boundary, whereas a single random field should be used in case of a soft boundary. Furthermore, this/these random field(s) can be cross-correlated with the domain indicators in order to account for edge effects, which may occur in the presence of both hard and soft boundaries.

In a nutshell, the geological domaining of a mineral deposit and the subsequent diagnosis of whether or not there exist clear-cut discontinuities across the domain boundaries have a great impact on modeling decisions and, therefore, on the prediction of properties relevant to the extraction or processing of the deposit. The presented exploratory tools allow the geologists and modelers to refine such a diagnostic on the basis of available sampling information and to avoid misinterpreting the nature of geological boundaries.

Acknowledgements

Mohammad Maleki and Xavier Emery acknowledge the funding of the Chilean Commission for Scientific and Technological Research, through grants CONICYT/FONDECYT/POSTDOCTORADO/N°3180655, CONICYT/FONDECYT/REGULAR/N°1170101 and CONICYT PIA AFB180004 (AMTC). The authors are also grateful to Prof. Brian Townley from University of Chile and two anonymous reviewers for helpful comments.

Appendix A. Proof of Eq. (7)

The cross-variogram between the indicator $I_{J,K}$ and the associated partial grade $Z_{J,K}$ is defined as

$$\gamma_{Z_{J,K}I_{J,K}}(\mathbf{h}) = \frac{1}{2}\mathbb{E}\{[Z_{J,K}(\mathbf{x}) - Z_{J,K}(\mathbf{x}+\mathbf{h})][I_{J,K}(\mathbf{x}) - I_{J,K}(\mathbf{x}+\mathbf{h})]\}. \tag{A1}$$

The increment $I_{J,K}(\mathbf{x}) - I_{J,K}(\mathbf{x}+\mathbf{h})$ is zero unless $\mathbf{x}$ belongs to D_J and $\mathbf{x}+\mathbf{h}$ to D_K or $\mathbf{x}+\mathbf{h}$ belongs to D_J and $\mathbf{x}$ to D_K. In any case, only one of the two partial grades $Z_{J,K}(\mathbf{x})$ and $Z_{J,K}(\mathbf{x}+\mathbf{h})$ is non-zero. It follows:

$$\begin{aligned}\gamma_{Z_{J,K}I_{J,K}}(\mathbf{h}) = {} & \tfrac{1}{2}\mathbb{P}\{\mathbf{x}\in D_J, \mathbf{x}+\mathbf{h}\in D_K\}\mathbb{E}\{Z(\mathbf{x})|\mathbf{x}\in D_J, \mathbf{x}+\mathbf{h}\in D_K\} \\ & + \tfrac{1}{2}\mathbb{P}\{\mathbf{x}\in D_K, \mathbf{x}+\mathbf{h}\in D_J\}\mathbb{E}\{Z(\mathbf{x}+\mathbf{h})|\mathbf{x}\in D_K, \mathbf{x}+\mathbf{h}\in D_J\}\end{aligned} \tag{A2}$$

where $\mathbb{P}(A)$ stands for the probability of event A. Under the additional assumption that $\mathbb{E}\{Z(\mathbf{x})|\mathbf{x}\in D_J, \mathbf{x}+\mathbf{h}\in D_K\} = \mathbb{E}\{Z(\mathbf{x}+\mathbf{h})|\mathbf{x}\in D_K, \mathbf{x}+\mathbf{h}\in D_J\}$, one obtains:

$$\gamma_{Z_{J,K}I_{J,K}}(\mathbf{h}) = \frac{\mathrm{P}\{\mathbf{x}\in D_J, \mathbf{x}+\mathbf{h}\in D_K\} + \mathrm{P}\{\mathbf{x}\in D_K, \mathbf{x}+\mathbf{h}\in D_J\}}{2}\mathbb{E}\{Z(\mathbf{x})|\mathbf{x}\in D_J, \mathbf{x}+\mathbf{h}\in D_K\} \tag{A3}$$

The same reasoning leads to

$$\gamma_{I_{J,K}\,I_{J,K}}(\mathbf{h}) = \tfrac{1}{2}\mathbb{P}\{\mathbf{x}\in D_J, \mathbf{x}+\mathbf{h}\in D_K\} + \tfrac{1}{2}\mathbb{P}\{\mathbf{x}\in D_K, \mathbf{x}+\mathbf{h}\in D_J\} \tag{A4}$$

The ratio $m_{J,K}(h) = \frac{\gamma_{Z_{J,K}\,I_{J,K}}(h)}{\gamma_{I_{J,K}}(h)}$ therefore takes the form given in Eq. (7).

Appendix B. Grade gradient across a boundary

Define δ_J as the cross-to-direct variogram ratio of the grade random field Z and the indicator I_J:

$$\delta_J(\mathbf{h}) = \frac{\gamma_{Z\,I_J}(\mathbf{h})}{\gamma_{I_J}(\mathbf{h})} \tag{B1}$$

The numerator is

$$\begin{aligned}\gamma_{Z\,I_J}(\mathbf{h}) &= \tfrac{1}{2}\mathbb{E}\{[Z(\mathbf{x})-Z(\mathbf{x}+\mathbf{h})][I_J(\mathbf{x})-I_J(\mathbf{x}+\mathbf{h})]\}\\ &= \tfrac{1}{2}\mathbb{P}\{\mathbf{x}\in D_J, \mathbf{x}+\mathbf{h}\notin D_J\}\mathbb{E}\{[Z(\mathbf{x})-Z(\mathbf{x}+\mathbf{h})]|\mathbf{x}\in D_J, \mathbf{x}+\mathbf{h}\notin D_J\}\\ &+ \tfrac{1}{2}\mathbb{P}\{\mathbf{x}+\mathbf{h}\in D_J, \mathbf{x}\notin D_J\}\mathbb{E}\{[Z(\mathbf{x}+\mathbf{h})-Z(\mathbf{x})]|\mathbf{x}+\mathbf{h}\in D_J, \mathbf{x}\notin D_J\}\end{aligned} \tag{B2}$$

$\mathbb{P}\{\mathbf{x}\in D_J, \mathbf{x}+\mathbf{h}\notin D_J\}$ and $\mathbb{P}\{\mathbf{x}+\mathbf{h}\in D_J, \mathbf{x}\notin D_J\}$ are always the same (Lantuéjoul, 2002). Thus, if $\mathbb{E}\{Z(\mathbf{x})-Z(\mathbf{x}+\mathbf{h})|\mathbf{x}\in D_J, \mathbf{x}+\mathbf{h}\notin D_J\}$ and $\mathbb{E}\{Z(\mathbf{x}+\mathbf{h})-Z(\mathbf{x})|\mathbf{x}+\mathbf{h}\in D_J, \mathbf{x}\notin D_J\}$ are equal, one has:

$$\begin{aligned}\gamma_{Z\,I_J}(\mathbf{h}) &= \mathbb{P}\{\mathbf{x}\in D_J, \mathbf{x}+\mathbf{h}\notin D_J\}\mathbb{E}\{[Z(\mathbf{x})-Z(\mathbf{x}+\mathbf{h})]|\mathbf{x}\in D_J, \mathbf{x}+\mathbf{h}\notin D_J\}\\ &= \gamma_{I_J}(\mathbf{h})\mathbb{E}\{[Z(\mathbf{x})-Z(\mathbf{x}+\mathbf{h})]|\mathbf{x}\in D_J, \mathbf{x}+\mathbf{h}\notin D_J\}\end{aligned} \tag{B3}$$

One finally obtains the cross-to-direct variogram ratio as the expected gradient of the grade across the boundary of domain D_J:

$$\delta_J(\mathbf{h}) = \mathrm{E}\{[Z(\mathbf{x})-Z(\mathbf{x}+\mathbf{h})]|\mathbf{x}\in D_J, \mathbf{x}+\mathbf{h}\notin D_J\} \tag{B4}$$

In a similar fashion, by restricting the analysis to $D_J \cup D_K$, one can analyze the gradient across the boundary between D_J and D_K:

$$\delta_{J,K}(\mathbf{h}) = \frac{\gamma_{Z_{J\cup K,\varnothing}\,I_{J,K}}(\mathbf{h})}{\gamma_{I_{J,K}}(\mathbf{h})} = \mathbb{E}\{[Z(\mathbf{x})-Z(\mathbf{x}+\mathbf{h})]|\mathbf{x}\in D_J, \mathbf{x}+\mathbf{h}\in D_K\}. \tag{B5}$$

Appendix C. Directional mean grade variation

Consider the non-centered cross-covariance between the indicator $I_{K,J}$ and the partial grade $Z_{J,K}$:

$$C_{I_{K,J}Z_{J,K}}(\mathbf{h}) = \mathrm{E}\{I_{K,J}(\mathbf{x})Z_{J,K}(\mathbf{x}+\mathbf{h})\} \tag{C1}$$

The product of the partial grade and the indicator is zero unless $\mathbf{x}$ belongs to D_K and $\mathbf{x}+\mathbf{h}$ belongs to D_J. Accordingly:

$$C_{I_{K,J}Z_{J,K}}(\mathbf{h}) = \mathbb{P}\{\mathbf{x}\in D_K, \mathbf{x}+\mathbf{h}\in D_J\}\mathbb{E}\{Z_{J,K}(\mathbf{x}+\mathbf{h})|\mathbf{x}\in D_K, \mathbf{x}+\mathbf{h}\in D_J\}. \tag{C2}$$

Likewise,

$$C_{I_{K,J}I_{J,K}}(\mathbf{h}) = \mathbb{P}\{\mathbf{x}\in D_K, \mathbf{x}+\mathbf{h}\in D_J\}. \tag{C3}$$

One finds out the mean grade variation $m_{J,K}(\mathbf{h})$ defined in Table 1 by dividing the two cross-covariances in Eqs. (C2) and (C3), but without any assumption of spatial symmetry.

Appendix D. Supplementary data

Supplementary data to this article can be found online at https://doi.org/10.1016/j.oregeorev.2020.103397.

References

Armstrong, M., Galli, A., Beucher, H., Le Loch, G., Renard, D., Doligez, B., Eschard, R., Geffroy, F., 2011. Plurigaussian Simulations in Geosciences. Springer, Berlin, pp. 176.

Bahar, A., Kelkar, M., 2000. Journey from well logs/cores to integrated geological and petrophysical properties simulation: a methodology and application. SPE Reservoir Eval. Eng. 3 (5), 444–456.

Chilès, J.P., Delfiner, P., 2012. Geostatistics: Modeling Spatial Uncertainty. Wiley, New York, pp. 699.

Clark, I., Basinger, K.L., Harper, W.V., 1989. MUCK – a novel approach to cokriging. In: Buxton, B.E. (Ed.), Proceedings of the Conference on Geostatistical, Sensitivity, and Uncertainty Methods for Ground-Water Flow and Radionuclide Transport Modeling. Battelle Press, pp. 473–493.

Dowd, P.A., 1993. Geological and structural control in kriging. In: Soares, A. (Ed.), Geostatistics Tróia' 92. Kluwer Academic, Dordrecht, The Netherlands, pp. 923–935.

Dowd, P.A., 1994. Geological controls in the geostatistical simulation of hydrocarbon reservoirs. Arab. J. Sci. Eng. 19 (2B), 237–247.

Dowd, P.A., 1997. Structural controls in the geostatistical simulation of mineral deposits. In: Baafi, E.Y., Schofield, N.A. (Eds.), Geostatistics Wollongong'96. Kluwer Academic, Dordrecht, The Netherlands, pp. 647–657.

Dubrule, O., 1993. Introducing more geology in stochastic reservoir modelling. In: Soares, A. (Ed.), Geostatistics Tróia' 92. Kluwer Academic, Dordrecht, The Netherlands, pp. 351–361.

Duke, J.H., Hanna, P.J., 2001. Geological interpretation for resource modelling and estimation. In: Edwards, A.C. (Ed.), Mineral Resource and Ore Reserve Estimation – the AusIMM Guide to Good Practice. The Australasian Institute of Mining and Metallurgy, Melbourne, pp. 147–156.

Emery, X., 2005. Variograms of order ω: a tool to validate a bivariate distribution model. Math. Geol. 37 (2), 163–181.

Emery, X., González, K., 2007. Incorporating the uncertainty in geological boundaries into mineral resources evaluation. J. Geol. Soc. India 69 (1), 29–38.

Emery, X., Maleki, M., 2019. Geostatistics in the presence of geological boundaries: Application to mineral resources modeling. Ore Geol. Rev. 114, 103124.

Emery, X., Ortiz, J.M., 2005. Estimation of mineral resources using grade domains: critical analysis and a suggested methodology. J. S. Afr. Inst. Min. Metall. 105 (4), 247–255.
Emery, X., Robles, L.N., 2009. Simulation of mineral grades with hard and soft conditioning data: Application to a porphyry copper deposit. Comput. Geosci. 13 (1), 79–89.
Emery, X., Silva, D.A., 2009. Conditional co-simulation of continuous and categorical variables for geostatistical applications. Comput. Geosci. 35 (6), 1234–1246.
Freulon, X., de Fouquet, C., Rivoirard, J., 1990. Simulation of the geometry and grades of a uranium deposit using a geological variable. In: Proceedings of the XXII International Symposium on Applications of Computers and Operations Research in the Mineral Industry. Technische Universität Berlin, Berlin, pp. 649–659.
Glacken, I.M., Snowden, D.V., 2001. Mineral Resource Estimation. In: Edwards, A.C. (Ed.), Mineral Resource and Ore Reserve Estimation – the AusIMM Guide to Good Practice. The Australasian Institute of Mining and Metallurgy, Melbourne, pp. 189–198.
Goovaerts, P., 1997. Geostatistics for Natural Resources Evaluation. Oxford University Press, New York, pp. 483.
Lantuéjoul, C., 2002. Geostatistical Simulation: Models and Algorithms. Springer, Berlin, pp. 256.
Larrondo, P., Leuangthong, O., Deutsch, C.V., 2004. Grade estimation in multiple rock types using a linear model of coregionalization for soft boundaries. In: Magri, E., Ortiz, J., Knights, P., Henríquez, F., Vera, M., Barahona, C. (Eds.), Proceedings of the First International Conference on Mining Innovation. Gecamin Ltda, pp. 187–196.
Larrondo, P., Deutsch, C.V., 2005. Accounting for geological boundaries in geostatistical modeling of multiple rock types. In: Leuangthong, O., Deutsch, C.V. (Eds.), Geostatistics Banff 2004. Springer, Dordrecht, The Netherlands, pp. 3–12.
Le Blévec, T., Dubrule, O., John, C.M., Hampson, G.J., 2018. Geostatistical modelling of cyclic and rhythmic facies architectures. Math. Geosci. 50 (6), 609–637.
Maleki, M., Emery, X., 2015. Joint simulation of grade and rock type in a stratabound copper deposit. Math. Geosci. 47, 471–495.
Maleki, M., Emery, X., 2017. Joint simulation of stationary grade and non-stationary rock type for quantifying geological uncertainty in a copper deposit. Comput. Geosci. 109, 258–267.
Maleki, M., Emery, X., Mery, N., 2017. Indicator variograms as an aid for geological interpretation and modeling of ore deposits. Minerals 7 (12), 241.
Mery, N., Emery, X., Cáceres, A., Ribeiro, D., Cunha, E., 2017. Geostatistical modeling of the geological uncertainty in an iron ore deposit. Ore Geol. Rev. 88, 336–351.
Ortiz, J.M., Emery, X., 2006. Geostatistical estimation of mineral resources with soft geological boundaries: a comparative study. J. S. Afr. Inst. Min. Metall. 106 (8), 577–584.
Patel, K.B., Pandalai, H.S., Subramanyam, A., 1996. Estimation of proportions of lithotypes using auxiliary information. Math. Geol. 28 (6), 765–781.
Rivoirard, J., 1993. Relations between the indicators related to a regionalized variable. In: Soares, A. (Ed.), Geostatistics Tróia'92. Kluwer Academic, Dordrecht, The Netherlands, pp. 273–284.
Rivoirard, J., 1994. Introduction to Disjunctive Kriging and Nonlinear Geostatistics. Clarendon Press, Oxford, pp. 192.
Rossi, M.E., Deutsch, C.V., 2014. Mineral Resource Estimation. Springer, Dordrecht, pp. 332.
Séguret, S.A., 2011. Block model in a multi facies context. Application to a porphyry copper deposit. In: Beniscelli, J. (Ed.), Proceedings of the Second International Seminar on Geology for the Mining Industry. Gecamin Ltda, Santiago, Chile, pp. 10.
Séguret, S.A., 2013. Analysis and estimation of multi-unit deposits: application to a porphyry copper deposit. Math. Geosci. 45 (8), 927–947.
Sinclair, A.J., Blackwell, G.H., 2002. Applied Mineral Inventory Estimation. Cambridge University Press, Cambridge, pp. 381.
Talebi, H., Lo, J., Mueller, U., 2017. A hybrid model for joint simulation of high-dimensional continuous and categorical variables. In: Gómez-Hernández, J., Rodrigo-Ilarri, J., Rodrigo-Clavero, M., Cassiraga, E., Vargas-Guzmán, J. (Eds.), Geostatistics Valencia 2016. Springer, Cham, pp. 415–430.
Talebi, H., Mueller, U., Tolosana-Delgado, R., van den Boogaart, K.G., 2019. Geostatistical simulation of geochemical compositions in the presence of multiple geological units: application to mineral resource evaluation. Math. Geosci. 51 (2), 129–153.
Tolosana-Delgado, R., Mueller, U., van den Boogaart, K.G., 2016. Compositionally compliant contact analysis. In: Raju, N. (Ed.), Geostatistical and Geospatial Approaches for the Characterization of Natural Resources in the Environment. Springer, Cham, pp. 11–14.
Vargas-Guzmán, J.A., 2008. Transitive geostatistics for stepwise modeling across boundaries between rock regions. Math. Geosci. 40 (8), 861–873.
Wilde, B.J., Deutsch, C.V., 2012. Kriging and simulation in presence of stationary domains: developments in boundary modeling. In: Abrahamsen, P., Hauge, R., Kolbjørnsen, O. (Eds.), Geostatistics Oslo 2012. Springer, Berlin, pp. 289–300.
Xu, C., Dowd, P.A., 2009. Conditional simulation of grades controlled by geological indicators. In: Dimitrakopoulos, R. (Ed.), Proceedings of the International Symposium on Orebody Modelling and Strategic Mine Planning. Australasian Institute of Mining and Metallurgy, pp. 43–50.
Yarus, J.M., Chambers, R.L., 1994. Stochastic Modeling and Geostatistics. Principles, Methods, and Case Studies. American Association of Petroleum Geologists, Tulsa, Oklahoma, pp. 409.